10.2 STATISTICAL ANALYSIS OF A RADAR-BASED ICING HAZARD ALGORITHM

Christopher J. Johnston [b]*, David J. Serke [b], David Albo [b], Andrew Weekley [b], Daniel R. Adriaansen [b], Scott M. Ellis [a], John C. Hubbert [a], Andrew L. Reehorst [c], Kim L. Elmore [d] and Marcia K. Politovich [b]

NCAR- National Center for Atmospheric Research
[a] Earth Observing Laboratory
[b] Research Applications Laboratory
Boulder, Colorado

[c] NASA- National Aeronautics and Space Administration Glenn Research Center
Cleveland, Ohio

[d] CIMMS- Cooperative Institute for Mesoscale Meteorological Studies
Norman, Oklahoma

1. INTRODUCTION

In-flight icing is considered one of the most dangerous weather conditions for pilots. Small amounts of ice on the surface of an aircraft can increase the amount of drag and decrease lift, which can cause hazardous flight conditions. Even though most commercial aircraft are now equipped with anti-icing devices, general aviation aircraft are less likely to have icing defense, and aircraft accidents have happened because the pilot chose to stay in icing conditions too long. The pilot must take evasive actions when icing conditions are observed.

Icing typically occurs when an aircraft ascends or descends through a layer of clouds or through precipitation that contains supercooled liquid water (SLW). SLW can be suspended in the atmosphere at temperatures below 0°C, until nearby ice crystals remove the liquid water from the air through the process of rapid evaporation and deposition onto the growing ice crystals, or through riming (Rogers and Floyd, 1989). As an airplane flies through areas of SLW, the SLW freezes upon contact with the leading edge of the wing and engine cowlings of the aircraft. Once the pilot has confirmed that icing is occurring, there are a few strategies that may be considered for extracting his or her craft from the hazardous conditions. These include ascending or descending from the cloud layer or simply turning around 180 degrees to leave these conditions. Pilots make voluntary reports (called PIREPs), on the presence or absence of in-flight icing conditions, and other weather-related conditions. Both a subjective icing severity ('trace', 'light', 'moderate', 'heavy' or 'severe') and icing type ('rime', 'clear' or 'mixed') may be included in each report. PIREPs are the only means of in-situ diagnoses of actual atmospheric conditions encountered by pilots and their aircraft in the absence of expensive icing research flights or specially instrumented fleet.

Over the past 30 years, advances in the diagnosis and detection of SLW have been made, including the development of the National Center for Atmospheric Research's (NCAR) Current/Forecast Icing Products and the National Aeronautics and Space Administration (NASA) Icing Remote Sensing System (NIRSS) (Reehorst et al., 2005). NIRSS (shown in Figure 1) is a vertically pointing prototype system that utilizes a Radiometrics Corporation 23-channel radiometer, a Vaisala laser ceilometer and a Metek Corporation K_a-band cloud radar.

The radiometer uses K-band brightness temperatures to derive integrated liquid water (ILW) and integrated water vapor amounts. The radiometer then uses the V-band to derive an atmospheric temperature profile (Solheim et al., 1998) by using an inversion method on a database of 10,000 radiosondes launched from the site nearest the radiometer's location and then training a neural network. NIRSS utilizes the ceilometer and the K_a-band cloud radar to define cloud base and top heights. NIRSS combines the input fields from each of the 3 sensors using fuzzy logic (a form of mathematical logic in which truth can assume a continuum of values between 0 and 1), and

**Corresponding author address: Christopher J. Johnston, National Center for Atmospheric Research, PO Box 3000, Boulder, CO 80307, chrisj@ucar.edu*

information gained from previous flight campaigns to distribute the detected ILW within the cloud.

Figure 1. *Image of the NIRSS hardware located at the NASA Glenn Research Center in Cleveland, Ohio.*

Theoretical studies and analyses using research radars (Vivekanandan et al., 1999, Ellis et al., 2001, Ikeda et al., 2008, Plummer et al., 2010, Hubbert et al., 2010, and Serke et al., 2012) have strongly suggested that the use of dual-polarization radar moment fields could provide better real-time diagnosis of in-flight icing conditions. Dual-polarization radar measurements provide information on the shape of the hydrometeor – liquid drop or ice/snow crystal – and thus, if the shape is known, inferences can be made about the potential of the sensed cloud or precipitation to produce icing conditions. Therefore, utilizing the Next-Generation radar (NEXRAD) upgrade to dual-polarization is a natural path for improved sensing of in-flight icing conditions. The polarized radar process is described in detail in Ellis et al. (2001). With the progression of operational radar technology to dual-polarization, there will come a need for operational polarized products. As it stands now, the research community has conceived no operational polarized icing products. An operational icing hazard detection algorithm would be the first of its kind.

NCAR recently developed a preliminary version of an Icing Hazard Level Algorithm (IHLA, Albo et al., 2012) that utilizes dual-polarimetric radar data and has been tested on data from the Colorado State University/University of CHicago, ILLinois (CSU-CHILL) scanning 10-cm wavelength S-band polarized radar located in Greeley, Colorado. The goal of this project was to see if the IHLA could detect the presence or absence of in-flight icing cases. The initial results from Albo et al. (2012) are promising; however this technique has not yet been applied to operational NEXRAD data.

The main objective of this project was to evaluate improvements in icing diagnosis resulting from operational dual-polarization parameters, and to establish the feasibility of using dual-polarization NEXRAD from Cleveland, Ohio's radar (KCLE) for icing diagnosis. Other objectives included exploring how the S-band freezing drizzle and mixed phase icing modules of the IHLA behaved under varying icing conditions. Furthermore, comparisons were made against NIRSS, which was located within 250 meters of KCLE. The study looked at a series of icing and non-icing cases based upon PIREPs inside a 50 km radius of KCLE from 27 January 2012 to 20 March 2012.

2. BACKGROUND

The detection of SLW and thus in-flight icing conditions with radar alone is a challenging prospect. By definition, SLW droplets have diameters that are < 50 μm and have low reflectivity (dBZ) values when viewed with NEXRAD. Liquid drops comingled with ice crystals (mixed phase conditions) create an even greater problem due to the fact that the ice crystals can dominate the backscatter radar signatures due to their generally larger size (Rinehart, 2010).

Since the end of 2011, the United States National Weather Service has begun a program to retrofit the network of S-band NEXRAD radars to include dual-polarimetric capabilities. Polarimetric radars transmit and receive both horizontally and vertically polarized radiation, which offers a more thorough depiction of hydrometeors than conventional NEXRAD radars. This gives scientists several polarized moment fields that quantify the vertical and horizontal properties of hydrometeors. These moment fields include: differential reflectivity (Z_{DR}), specific differential phase (K_{DP}), linear depolarization ratio (LDR), cross-correlation coefficient (ρ_{HV}), and different propagation phase (Φ_{DP}). These moment fields are described in detail in Doviak and Zrnić (1993, chapter 8). Analyses using dual-polarization moment fields have indicated that both small droplets and asymmetrical, randomly orientated ice crystals are classified by Z_{DR} and K_{DP} near zero.

Several studies over the past 15 years have researched ways to detect the presence of SLW within clouds using radar. The first of these studies performed by Vivikanandan et al. (1999), describe a fuzzy logic-based method for a particle classification technique that made use of polarimetric radar

observations. As stated earlier, fuzzy logic is a form of mathematical logic in which truth can assume a continuum of values between 0 and 1. The fuzzy boundaries between polarimetric observables are ideally suited for a fuzzy logic-based particle classification approach (Vivikanandan et al., 1999). Using microphysical characteristics of hydrometeors, such as size, shape, orientation relative to the local vertical direction, phase (liquid or ice), and bulk density (wet, dry, aggregate, or rimed), Vivekanandan et al. created fuzzy logic membership functions for different hydrometeor types (Figure 2).

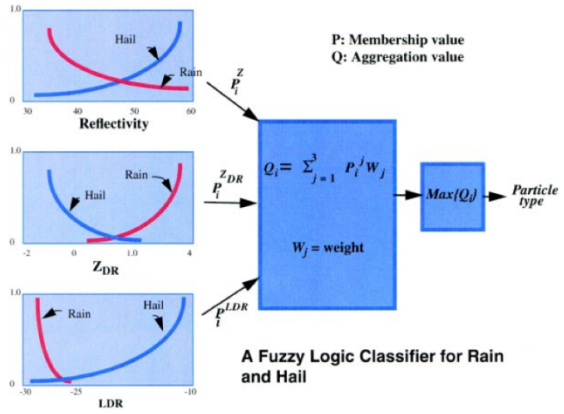

Figure 2. *An example of a fuzzy logic particle identification algorithm. For each variable, all of the particles receive a value between 0 and 1 from the respective membership function (fuzzification). These values (**P**) are then multiplied by the appropriate weight (**W**) and summed for each particle. The maximum of the weighted sums is then found to determine the particle type (Vivekanandan et al., 1999).*

The result of this effort was the development of one of the first Particle IDentification (PID) algorithms (labeled by the research community as the 'legacy' PID) based upon dual-polarization moment fields. The algorithm worked best for warm season weather scenarios. One of the limitations of the PID was that a number of different species of hydrometeors have overlapping classification signatures in polarized moment fields. This classification problem occurs mostly with cold season mixed phase conditions.

Studies completed by Elmore (2009) and Park et al. (2009) recognized that further research would need to be completed on hydrometeor classification algorithms (HCA) especially in cold season cases. Elmore evaluated the National Severe Storms Laboratory's (NSSL) HCA, which was designed for warm season use with the polarimetric upgrade of the NEXRAD radars. The study utilized reports of surface precipitation type, collected by educated residents in the Oklahoma City area from the winter of 2006-2007, and compared them to HCA output from the lowest KOUN S-band tilt. Elmore calculated a Pierce Skill Score (Joliffe and Stephenson, 2003; Wilks, 2006) of 0.115, which corresponded to the HCA accurately discriminating between no, frozen and liquid surface precipitation only 11.5 % of the time. Elmore concluded, "In its current form, HCA performance is probably not suitable for determining hydrometeor type near the ground in winter precipitation." Researchers continued to work on techniques to classify wintertime hydrometeors.

Both snow and freezing drizzle characteristically have reflectivities that are similar (< 5 dBZ), are spatially analogous and are hard to differentiate amongst one another. Ikeda et al. (2008) found that NEXRAD reflectivity could be used to detect the presence of freezing drizzle at the lowest radar elevations. Ikeda et al. noticed that clouds producing freezing drizzle at the surface had smoother radar reflectivity than those that produce snow. Furthermore, Ikeda et al. explained that drizzle characteristic patterns differ from light snow due to the occurrence of snowbands, ice-generating cells, and higher vertical reflectivity gradients correlated with ice particle growth process. Using local and global standard deviations and reflectivity texture weighted with a fuzzy-logic scheme, an algorithm was created. The study showed that the algorithm was able to distinguish between these two particle types for 70% of their total observations of drizzle.

Another recent study suggested that the detection of SLW with radar was possible (Plummer et al., 2010). This study was completed during the Mesoscale Alpine Programme in the Italian Alps with the National Science Foundation's polarized S-band research radar and the Electra weather research aircraft. Both aircraft measurements of microphysical properties using particle probes and dual-polarization measurements of these clouds were made. This study's primary goal was to examine polarization radar signatures associated with SLW in orographic cloud systems of northern Italy and quantify their use as probabilistic remote SLW identification criteria. The analysis revealed that mean values of Z_{DR} and K_{DP} were greater in regions of ice-only as compared to mixed phase, and that the variance of Z_{DR} and K_{DP} were also greater in regions of ice-only as compared

to mixed phase. The outcome of the study was the observation of the Z_{DR} and K_{DP} relationships during mixed phase and a probability distribution of SLW within clouds using polarization moment fields. This lead to the beginning of research into classifying hydrometeors aloft, since previous HCA's only detected precipitation types at the surface.

Since 2010, aircraft icing researchers at NCAR have made several advancements on the classification of hydrometeors aloft. This research was begun with the utilization of spatial statistics of polarized moment fields on a tilt-by-tilt basis. This method employs observations by numerous research groups (Vivekanandan et al., 1999, Ikeda et al., 2008, Plummer et al., 2010 and Williams et al., 2011) on the indirect (not absolute gate-by-gate values) moment measurements. The resulting IHLA (Albo et al., 2012) was developed during the winter season of 2010/2011. During NCAR's development of IHLA, dual-polarization radar data sets from CSU-CHILL were collected during in-flight icing conditions. NIRSS was relocated from Cleveland, Ohio to the National Oceanic and Atmospheric Administration (NOAA) Platteville field site in early November 2010. The NOAA Platteville field site was located at a range of 30.2 km to the south-southwest of CSU-CHILL and 36.2 km to the north-northeast of Denver International Airport (KDEN) (Figure 3).

Data gathered for this project were validated using PIREPs of icing conditions and NIRSS observations. NIRSS has been shown to have good skill in discriminating and quantifying cloud liquid water (Reehorst et al., 2006 and Johnston et al., 2011) and thus, for the project, was used as verification for the IHLA.

Using the dual polarimetric radar volume datasets from CSU-CHILL and Weather Research and Forecast Rapid Refresh (WRF-RR) model temperature profiles centered over the grid point of CSU-CHILL, for several icing and non-icing cases (as verified by PIREPs and NIRSS), a series of algorithms were built/modified, which make up the IHLA (Figures 4 and 5). First, a FreeZing Level Algorithm (FRZLA) based upon previous works by Gourley and Calvert (2003) and Brandes and Ikeda (2004), was constructed. The freezing level as defined by Glickman (2000) is the lowest level in the atmosphere at which the temperature, measured by a thermometer exposed to the air, is 0°C.

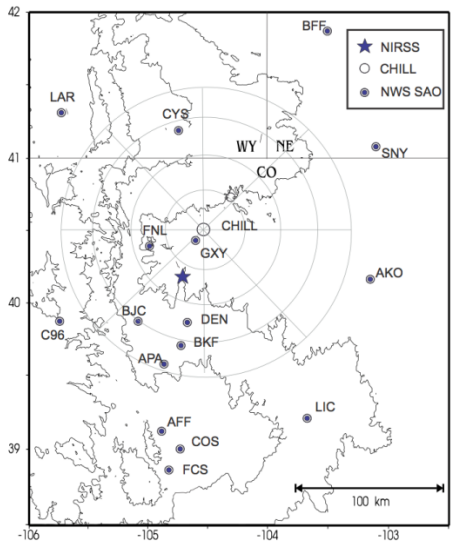

Figure 3. *Map of the Front Range of Colorado, showing the location of CSU-CHILL, NIRSS and National Weather Service Surface Atmospheric Observations (NWS SAO). Range rings around CSU-CHILL are at 25-km intervals. Terrain contours start at 5,000 feet MSL with 2,000-foot increments (Albo et al., 2012).*

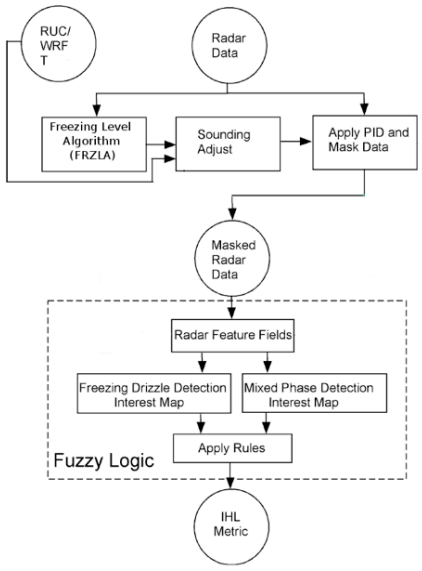

Figure 4. *Flow diagram of the IHLA (Albo et al., 2012).*

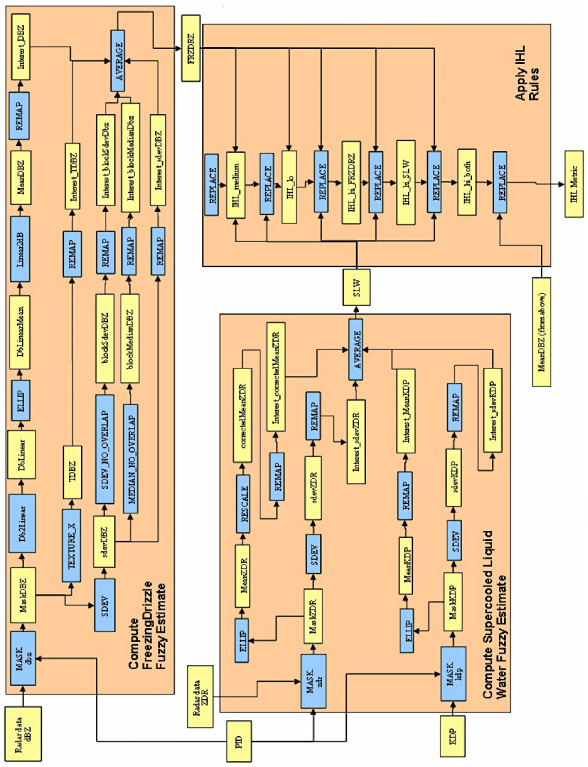

Figure 5. *Detailed flow diagram for the IHLA. The freezing drizzle (MNDDA, referred to as FRZDRZ within IHLA) algorithm is at the top; the supercooled liquid (SLWA, referred to as SLW within IHLA) algorithm is at bottom left; the final IHLA calculation is at bottom right. This diagram is available online at http://rap.ucar.edu/projects/IHLA/IHLAlgorithm/Page 1.html (Albo et al., 2012).*

The FRZLA uses bright band (the enhanced radar reflectivity echo of snow as it melts to rain) detection and Numerical Weather Prediction (NWP) model freezing level heights as a basis for where the freezing level is located. FRZLA derives full or partial rings of the polarized moment fields and then assigns the freezing level to the lowermost height of the detected ring. Next, the radar-derived bright band height is used in IHLA to adjust the WRF-RR model temperature profile.

After this, the PID algorithm based on Vivekanandan et al. (1999) was utilized. The PID is run on a radar volume and all non-weather (birds, bugs, clutter, etc.) and non-freezing particle types are masked out. Next, the masked radar moment fields are applied by two different meta-algorithms for detecting freezing drizzle and mixed phase areas. The two meta-algorithms are a modified version of the Ikeda et al., 2008-based NEXRAD Drizzle Detection Algorithm (MNDDA, referred to as FRZDRZ within IHLA) and a Supercooled Liquid Water Algorithm (SLWA, referred to as SLW within IHLA) based on Plummer et al. (2010).

The FRZDRZ algorithm calculates numerous statistical measures (or feature fields) and uses fuzzy logic to convert these measures into scores; the individual scores are then combined into a single final score. If the final score is above a specific threshold, freezing drizzle is inferred to be present in the scan. The statistical measures calculated are the median reflectivity, the global standard deviation of the reflectivity, the median of the local standard deviation of the reflectivity, the standard variation of the local standard deviation of the reflectivity, and the median reflectivity of the local texture (Figure 6).

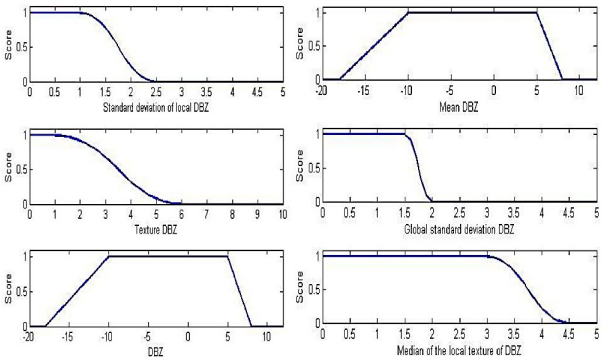

Figure 6. *FRZDRZ membership functions (Albo et al., 2012).*

The feature fields used in the SLW algorithm are computed over a local area and include the mean of Z_{DR}, standard deviation of Z_{DR}, mean of K_{DP} and the standard deviation of K_{DP}. Membership functions similar to those described in the FRZDRZ algorithm were designed and applied to produce interest values (Figure 7, next page). Next, the four interest values were combined into a weighted sum and normalized to obtain an output from 0 to 1, with 0 suggesting no likelihood of icing and 1 a high likelihood of icing.

The final IHLA output is a combination of the resulting interest fields from the two meta-algorithms FRZDRZ and SLW. The icing hazard values are scaled from 0.0 to 1.0, with 0.0 being 'no icing', 0.5 being 'maybe icing' and 0.7 to 1.0 being 'yes icing' (see Table 1, section 8.3). The values from 0.7 to 1.0 termed 'yes icing' include high FRZDRZ output (icing hazard value of 0.7, named 'FRZDRZ yes'), high SLW output (icing hazard value of 1.0, named

'SLW yes') and both high FRZDRZ and SLW (icing hazard value 0.8). Since IHLA is a newly made algorithm, it is going to take time to modify before the algorithm can become operational. Therefore, the algorithm is not going to be ideal and errors will need to be sought out.

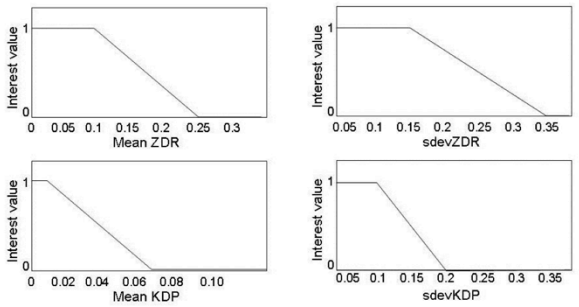

Figure 7. *Membership functions within the SLW for mean (left) and standard deviation (right) of Z_{DR} (top) and K_{DP} (bottom) (Albo et al., 2012).*

In weather situations where only small, non-precipitating SLW drop sizes exist; S-band radars will detect nothing, as the returned signal would be below the radar's signal-to-noise ratio. These situations, such as freezing fog, are not unusual across the northern US in winter. This is furthermore proven based upon limitations due to the radar cross-section (RCS) of a droplet (Figure 8) (Rinehart, 2010).

$$\textbf{Radar Cross Section} - \textbf{Single Droplet}$$

$$\sigma_{drop} = \frac{C\pi^5 D^6}{\lambda^4}$$

$$C = 1.00\ for\ liquid\ water\ \&\ \sim 0.2\ for\ ice\ water$$

$$D = Diameter\ of\ hydrometeor$$

$$\lambda = Wavelength\ of\ radar\ (S - band\ \sim 10^{-1} m)$$

Figure 8. *Radar cross-section (RCS) for a single droplet, η units of m^2m^{-3} (information from Rinehart, 2010).*

The reflectivity of volume clutter (such as SLW) is characterized in terms of an RCS per unit volume η (units of m^2m^{-3}). As indicated before, SLW droplets have diameters < 50 μm ($5 \times 10^{-5}\ m$). Even if a SLW droplet is ≈ 50 μm in diameter, the RCS of the droplet is a meager $5 \times 10^{-20} m^2 m^{-3}$, as compared to a normal continental rain droplet ($\approx\ 2 \times 10^{-3}\ m$ in diameter), that has an RCS of $2 \times 10^{-10} m^2 m^{-3}$. Previous work by Hubbert et al. (2010, parts 1 and 2) describe how non-zero mean canting angle of ice crystals cause biases in the Z_{DR} field due to cross-coupling. This occurs with the simultaneous transmitted horizontal and vertical power in the operational radars (such as dual-polarized NEXRAD), but not in the fast alternating system employed by research S-band radars. Furthermore, Z_{DR} cannot be calibrated by performing vertical scans with NEXRAD as is done with research radars, since NEXRAD radars cannot vertically point the antenna.

3. DATA AND METHODOLOGY

3.1 Data Sources

There were numerous data sources for this project. As noted earlier, the inputs to IHLA are dual-polarized radar volume scans and NWP model data from the WRF-RR. When input into the IHLA, the radar data was assumed to have been processed with an algorithm such as Clutter Mitigation Decision and a clutter filter such as Gaussian Model Adaptive Processing, which is used when producing level II NEXRAD data. The level II NEXRAD data for KCLE was retrieved from the National Climatic Data Center website for this project. The WRF-RR NWP was downloaded from the Mesoscale and Microscale Meteorology database, which was located on NCAR's Mass Storage System. Moreover, icing related PIREPs and NIRSS data was retrieved from their respective databases on NCAR's server network.

3.2 Methodology

3.2.1 Case Selections

Previous work with IHLA was limited to only a handful of known icing cases with research radars. In this work, the authors wanted to accomplish a more comprehensive survey of the first version of IHLA with operational radars. In order to have the greatest chance of succeeding in obtaining a broader understanding of the strengths and weaknesses of this early stage algorithm, the authors desired to start with a maximum number of candidate cases and then methodically pare away classes of cases that were not truly representative of icing or non-icing events with collocated PIREPs.

The authors began with two classes of cases in order to attempt to prove out IHLA: null or non-icing severity and moderate or greater icing severity within 100 km of KCLE. From there, 53 null cases and 47 moderate or greater cases were found within the 2-

month span from late January to late March. The null cases were reduced to 45 when only cases with significant radar return existed in the volume. PIREPs are sometimes reported out of precipitating and even cloudy regions when turbulence is reported or in a region where a pilot knows weather has been reported recently. Null PIREPs can also be reported at extremely high altitudes when a pilot reports on a condition other than icing, such as turbulence or clouds within the area of the flight. High altitude null PIREPs were discarded from study, which brought the total null cases down to 39. Next, cases from both categories were neglected if there were radar artifacts seen in the total volume, since these created a false report of IHLA 'yes icing'. These artifacts included sun echoes and radar beam blockages that were likely caused by objects near the KCLE radar. This downgraded the case totals for each to 36 for the null cases and 44 for the moderate or greater cases. Furthermore, missing radar data for a series of cases was noted, and these were abandoned from the study. The totals for both the null and moderate or greater cases were identical after the missing radar data cases were discarded, with 32 cases for each. To ensure representativeness, the authors reduced the case search parameters to within 50 km of KCLE. This reduced the field of null cases to 17 and moderate or greater to 14, however the authors feel that having fewer cases to compare was not as much of a risk than to include cases in the two categories that do not truly represent the intended scenario.

3.2.2 Running IHLA

After the representative cases were collected, PIREPs were matched to polarimetric radar volumes from KCLE with the closest time. A mean time difference of ± 6.0 minutes occurred between the moderate or greater PIREP times and the respective radar volume time. For null PIREP times, a mean time difference of ± 4.76 minutes occurred between the PIREP time and the radar volume time. Next, both radar volumes and WRF-RR model sounding data for the grid point above KCLE were downloaded and the IHLA was run. The resulting IHLA output fields were ingested into a plotting program that mapped each radar tilt for all the characteristic fields.

3.2.3 Polarimetric Radar Volume Analysis

For the KCLE IHLA radar volume analysis, the total number of radar pixels for each of the IHLA output fields per volume were divided by the total pixels in the volume that had returned power above the signal-to-noise level. This created a percentage of IHLA 'yes icing', IHLA 'maybe icing' and IHLA 'no icing' for each individual case. To get the total percentages for all the null and moderate or greater cases, the pixels where IHLA was yes (including the fields 'FRZDRZ yes' and 'SLW yes'), no and maybe were summed and divided by the sum of the total radar return pixels above the threshold individually for null cases, then moderate or greater cases. The total results for both null and moderate or greater icing cases were recorded then averaged. The total results are discussed in section 4.2.1. Furthermore, individual case studies that were characteristic of the total radar volume analysis study are described in section 4.1 for both a null and moderate or greater icing case.

3.2.4 NIRSS Comparison Analysis

NIRSS data provides a valuable independent measurement of SLW that can be compared and verified to the results of the IHLA. There are several advantages to using the NIRSS radiometer measurements of ILW, although, there are particular disadvantages too. The comparisons with the radiometer have the advantage that the radiometer measurements are available at a known location for long periods of time enabling analysis in various conditions. One of the disadvantages was that NIRSS was in the cone of silence of the KCLE polarimetric radar. Therefore, there was not polarimetric radar data available above the site; however, the atmospheric environment near NIRSS was fairly representative of the 50 km study radius, especially since most of the cases were of winter stratiform type. The radiometer measurements also have the disadvantage of measuring ILW values, meaning the authors could not know at what vertical levels the measured liquid was located. NIRSS does include algorithms that distribute the liquid water into the clouds according to cloud top temperature and reflectivity; however, this feature was not used in the comparisons. There was also no way to know if the liquid that was detected was mixed with ice particles.

During this part of the analysis, the authors matched all the representative icing and non-icing mean radar volume percentages for IHLA 'yes icing' (section 3.2.3) for each individual case to 5-minute mean ILW values of NIRSS. To do this, times were selected halfway between the time of the PIREP and the time of the polarimetric radar volume scan. If the times were not exactly halfway between the two, a time was chosen nearer to the time of the PIREP.

Next, 5-minute averages of ILW were made centered on the halfway time. Lastly, the individual mean radar volume percentages for IHLA 'yes icing' were matched and plotted for null and moderate or greater icing cases. The results of the ILW comparisons to volumetric statistics are detailed in section 4.2.2. Additionally, the times, values of the 5-minute mean ILW from the NIRSS radiometer, and the mean volume percentages for each case are provided for reference in the Appendix 8.3 for both null and moderate or greater icing cases.

4. RESULTS AND DISCUSSION

4.1 Case Studies

Two case studies are presented here to illustrate the results of the IHLA for representative cases of moderate and null PIREPs. In each case, a synoptic weather analysis, current condition evaluation, an analysis of IHLA's output of reflectivity, icing hazard module, freezing drizzle and mixed phase icing modules, and a evaluation of NIRSS's 5-minute mean ILW value are discussed. The input and output fields will be examined to determine how they match the conceptual models of in-flight icing environments. In addition, strength and weaknesses of the algorithm will be reviewed. In both cases the KCLE NEXRAD was operated in clear air mode. NIRSS was also in a vertically pointing mode.

4.1.1 Moderate PIREP Case: 1408 UTC 02 February 2012

At 1400 UTC 02 February 2012, a surface low was moving across the central Appalachians, which was bringing moisture to the mid-Atlantic region. A cold front was moving in from the northeast, while Cleveland, Ohio was ahead of the front (1500 UTC analysis is shown in figure 9). This cold front caused instability ahead of it, and clouds were shrouding Cleveland. Flow from the north-northwest was moving cold air across an unfrozen Lake Erie, which also provided airmass instability. The temperature at KCLE at the time of the PIREP (1408 UTC) was 2.7°C (37°F). Less than an hour later at 1500 UTC, infrared satellite imagery showed that cloud top temperatures over the Cleveland area were between -5 and -15°C (color scale, Figure 9). This temperature range has been shown in previous research to be conducive for SLW formation in clouds (Rogers and Floyd, 1989).

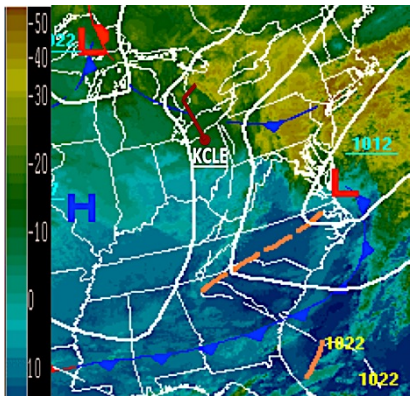

Figure 9. *Zoomed in 1500 UTC surface pressure (yellow lines, [hPa]), cloud top temperature (color bar, [°C]), and frontal analysis for 02 February 2012. Wind barb shown in dark red. (Hydrometeorological Prediction Center, 2012).*

Figure 10 (top of next page) displays KCLE radar reflectivity and IHA output for the 0.5-degree elevation scan. Range rings were superimposed over the plots at 25 km increments. The 50 km ring is shown in red, as this was the radius of the icing case search as detailed in section 3.2.1. A Cartesian coordinate grid with units in kilometers was also superimposed over the plots, with KCLE centered at the origin. The IHLA output plot on the right in Figure 10, has a color bar that corresponds to different icing hazard values, as discussed in section 2. Blue colors correspond to an icing interest of 0.0, which means that none of the interest thresholds for mixed phase SLW or freezing drizzle were exceeded at a given pixel. Green colored pixels correspond to an icing interest of 0.5, which means that at least some of the fields that go into the SLW or freezing drizzle calculations were close to but not exceeding thresholds for 'yes icing'. Lastly, any icing value above 0.7 is considered to be in the 'yes icing' category, since the SLW and freezing drizzle categories of IHLA are designed to detect several different in-flight icing scenarios. Orange colored pixels correspond to interest fields for the freezing drizzle detection exceeding thresholds for icing detection. Maroon colored pixels correspond to interest fields for SLW detection exceeding thresholds for icing detection, and bright red pixels mean both SLW and freezing drizzle criteria were met. In all cases studied to date, very few pixels are ever categorized as 'both', lending credence to the assertion that these two detection algorithms are correctly sensing disparate scenarios (Serke et al., 2012).

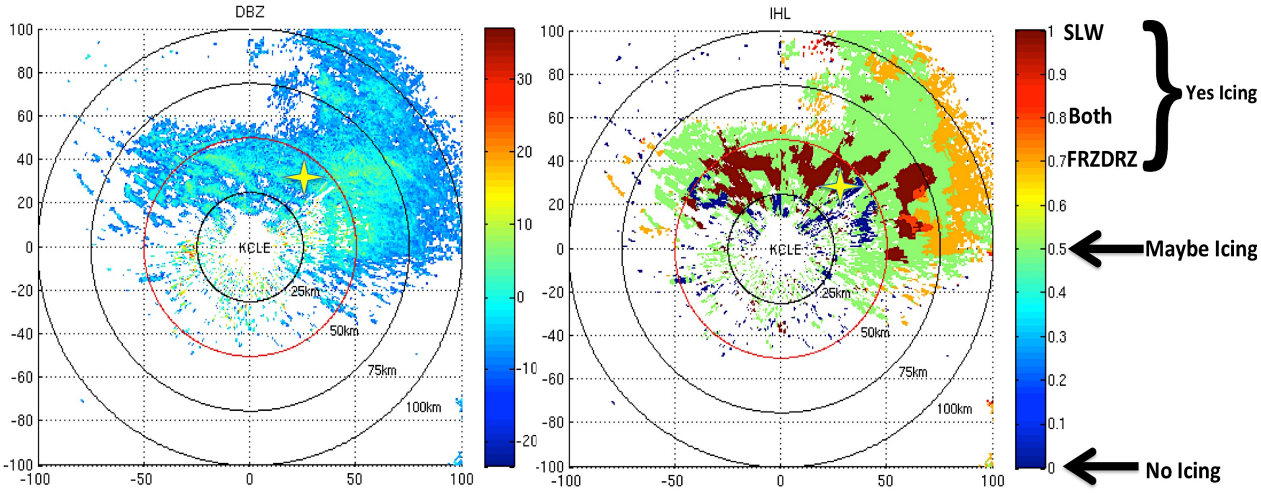

Figure 10. *KCLE NEXRAD reflectivity from elevation 0.5 degrees (left) and KCLE IHLA output for elevation 0.5 degrees (right) from 1413 UTC 02 February 2012. The x-y axes are in km from the KCLE radar and NIRSS. PIREP location is shown as a gold star.*

KCLE radar reflectivity values between -10 and 10 dBZ were seen north and east of KCLE (Figure 10). The IHLA output at the 0.5 degree elevation scan showed significant areas of 'maybe icing', and 'yes icing'. There were also smaller areas of 'no icing'. Significant areas of 'SLW yes' were shown, as well as small areas having both 'SLW yes' and 'FRZDRZ yes'. For this case, the mean volume percentage of 'yes icing', 'SLW yes', 'FRZDRZ yes', 'maybe icing', and 'no icing' were: 44.7 %, 31.5 %, 13.2 %, 49.7 % and 5.60 %, respectively. As stated in section 2, the 'yes icing' category is made up of both 'SLW yes' and 'FRZDRZ yes', so these percentages combine to make the total percentage of the 'yes icing' category.

The PIREP location was approximately 38 km to the northeast of KCLE, at an altitude of around 1829 meters (6,000 feet) above mean sea level (MSL) (the PIREP text is shown in section 8.2.2). This corresponded to an elevation angle scan of 2.4 degrees on the KCLE radar according to Figure 11. The nearest elevation angle to this was the 2.5 degree scan. If the PIREP flight level and location were correctly reported, this would have put the aircraft just outside of an area of 'SLW yes', as shown on the IHLA 2.5 degree elevation angle scan output (Figure 12, top of next page). As stated before, infrared satellite imagery showed that at 1500 UTC, about an hour after the PIREP, that the cloud top temperature near Cleveland was between -5 and -15°C.

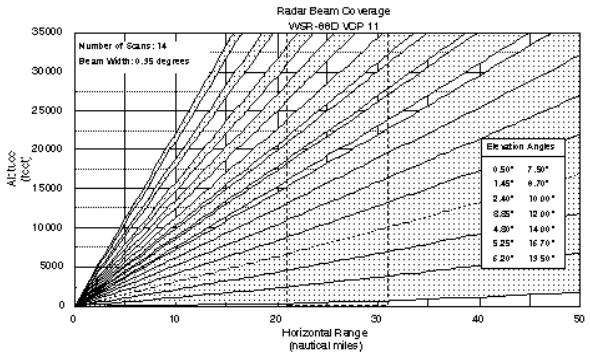

Figure 11. *Range versus height plot of a typical WSR-88D/NEXRAD VCP (Wheeler, 1997).*

These conditions were ideal for SLW. Furthermore, NIRSS's 5-minute mean ILW value at 1411 UTC was 0.432 gm^{-3}, which corresponded to a NIRSS icing severity of heavy (Table 3, section 8.3). Overall, the IHLA output near the location of the PIREP and mean warning volume percentages looked to correspond with the known icing conditions seen by the pilot. The SLW algorithm looked to be working correctly for this case. There was however, a large percentage of 'icing maybe', which should be looked at in a future analysis.

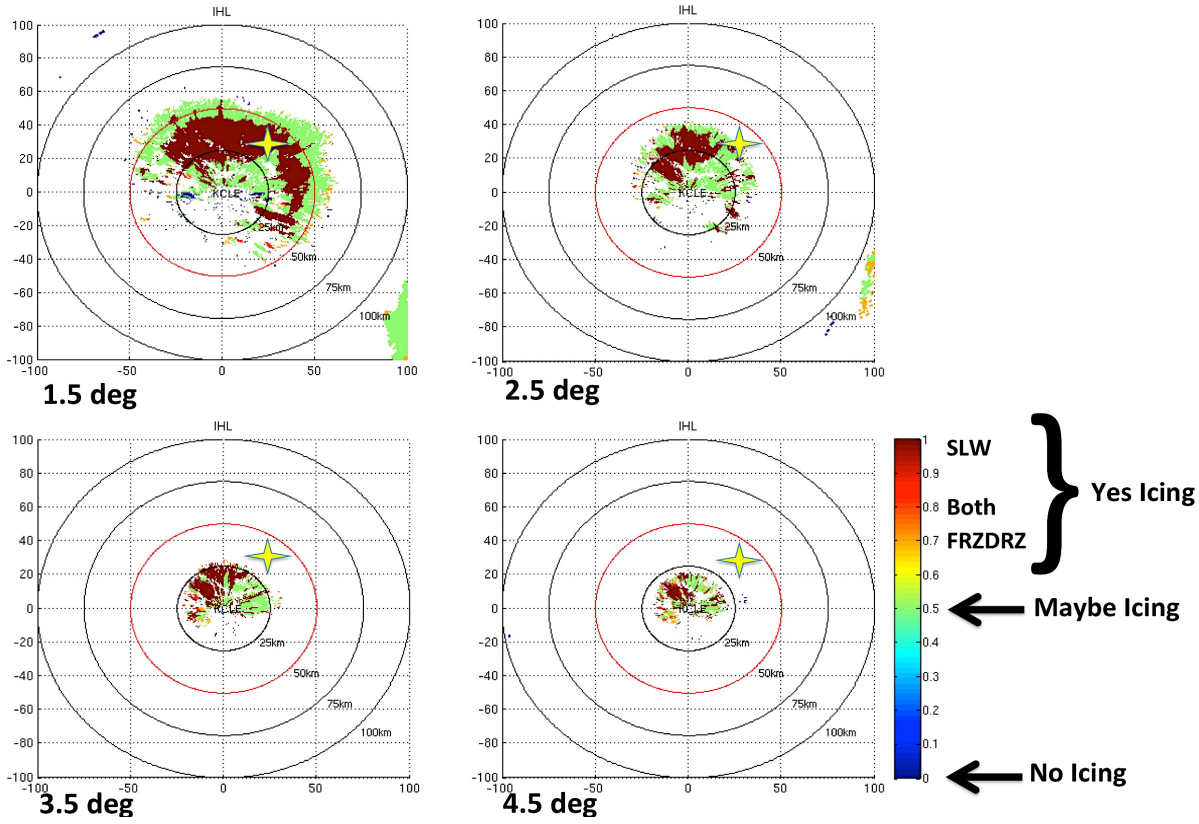

Figure 12. *KCLE IHLA output for elevations 1.5 to 4.5 degrees from 1413 UTC 02 February 2012. PIREP location is shown as a gold star.*

4.1.2 Null PIREP Case: 1721 UTC 12 February 2012

At 1800 UTC 12 February 2012, a shortwave trough not associated with any significant low-pressure system was northwest of Cleveland (Figure 13). This shortwave was embedded within the periphery of a high-pressure system that was dominant over much of the Midwest and the Mississippi valley. Flow was from the west-northwest with surface temperatures near -5°C (23°F) at Cleveland. This flow was moving the cold air over an unfrozen Lake Erie, which provided airmass instability. Moisture laden air came ashore, bringing clouds and light snow showers that developed due to lake-effect enhancement. At 1800 UTC, infrared satellite imagery showed that cloud top temperatures over the Cleveland area were between -20 and -30°C (color scale, Figure 13). These conditions were ideal for snow, as well as areas of ice crystals and SLW within the clouds aloft.

KCLE radar reflectivity at the 0.5 degree elevation scan had values between -5 and 20 dBZ, with some areas of reflectivity in the 20 to 30 dBZ range (Figure 14, left, bottom of next page).

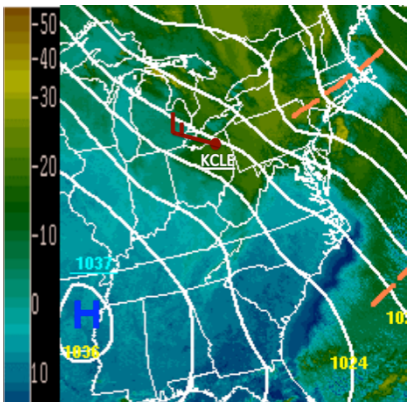

Figure 13. *Zoomed in 1800 UTC surface pressure (yellow lines, [hPa]), cloud top temperature (color bar, [°C]), and frontal analysis for 12 February 2012. Wind barb shown in dark red. (Hydrometeorological Prediction Center, 2012).*

There was a clear air pocket near KCLE at this time. Banding can clearly be seen in the 0.5 degree reflectivity to the west-southwest of KCLE, which is likely where snow was falling. Stronger areas of reflectivity (-20 to 30 dBZ) were seen from the east-northeast to the southeast of KCLE. The IHLA output at the 0.5 degree elevation scan showed substantial areas of 'maybe icing' and 'no icing', and smaller areas of 'SLW yes' and 'FRZDRZ yes' (Figure 14, right). The areas of stronger reflectivity were where areas of 'SLW yes' were seen on the IHLA output. Aloft in the 1.5 degree elevation scan (Figure 15, top of next page), the IHLA output displayed large areas of 'no icing' and 'maybe icing', as well as small areas of 'SLW yes'. The higher elevation scans showed nearly no areas of 'SLW yes', while areas of 'no icing' and 'maybe icing' became dominant. For this case, the mean volume percentage of 'yes icing', 'SLW yes', 'FRZDRZ yes', 'maybe icing', and 'no icing' were: 4.20 %, 3.14 %, 1.06 %, 45.8 % and 50.0 %, respectively.

The PIREP location was approximately 10 km to the southeast of KCLE, at an altitude of about 1219 meters (4,000 feet) MSL (the PIREP text is shown in section 8.2.1). This corresponded to an elevation angle scan of 4.8 degrees on the KCLE radar according to Figure 11. The nearest elevation angle to this was the 4.5 degree scan. If the PIREP flight level and location was accurately stated, this would have put the aircraft inside of an area of 'no icing', as shown on the IHLA 4.5 degree elevation angle scan output (Figure 15). As stated previously, infrared satellite imagery showed that at 1800 UTC, nearly an hour after the PIREP, that the cloud top temperature near Cleveland was between -20 and -30°C. In this case, the pilot reported an outside air temperature of -14°C, which would correspond to an area of either SLW or ice crystals. The pilot reported no icing and the IHLA output matched the condition. Moreover, NIRSS's 5-minute mean ILW value at 1724 UTC was 0.196 gm^{-3}, which corresponded to a NIRSS icing severity of light (Table 2, section 8.3).

In general, the IHLA output near the location of the PIREP and mean warning volume percentages looked to correspond with the known icing conditions seen by the pilot. However, similar to the last case, a large percentage of 'maybe icing' was seen, which should be looked at in a future analysis. NIRSS's icing severity of light did not agree with the PIREP, however, features of SLW and ice crystals aloft can move over the vertically pointing system and change the severity rather quickly.

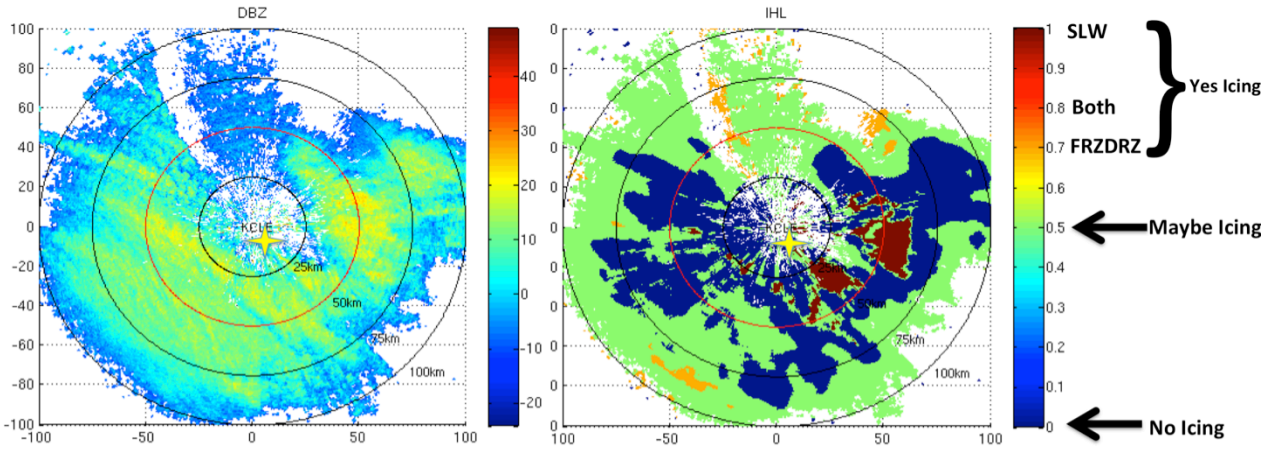

Figure 14. *KCLE NEXRAD reflectivity from elevation 0.5 degrees (left) and KCLE IHLA output for elevation 0.5 degrees (right) from 1728 UTC 12 February 2012. The x-y axes are in km from the KCLE radar and NIRSS. PIREP location is shown as a gold star.*

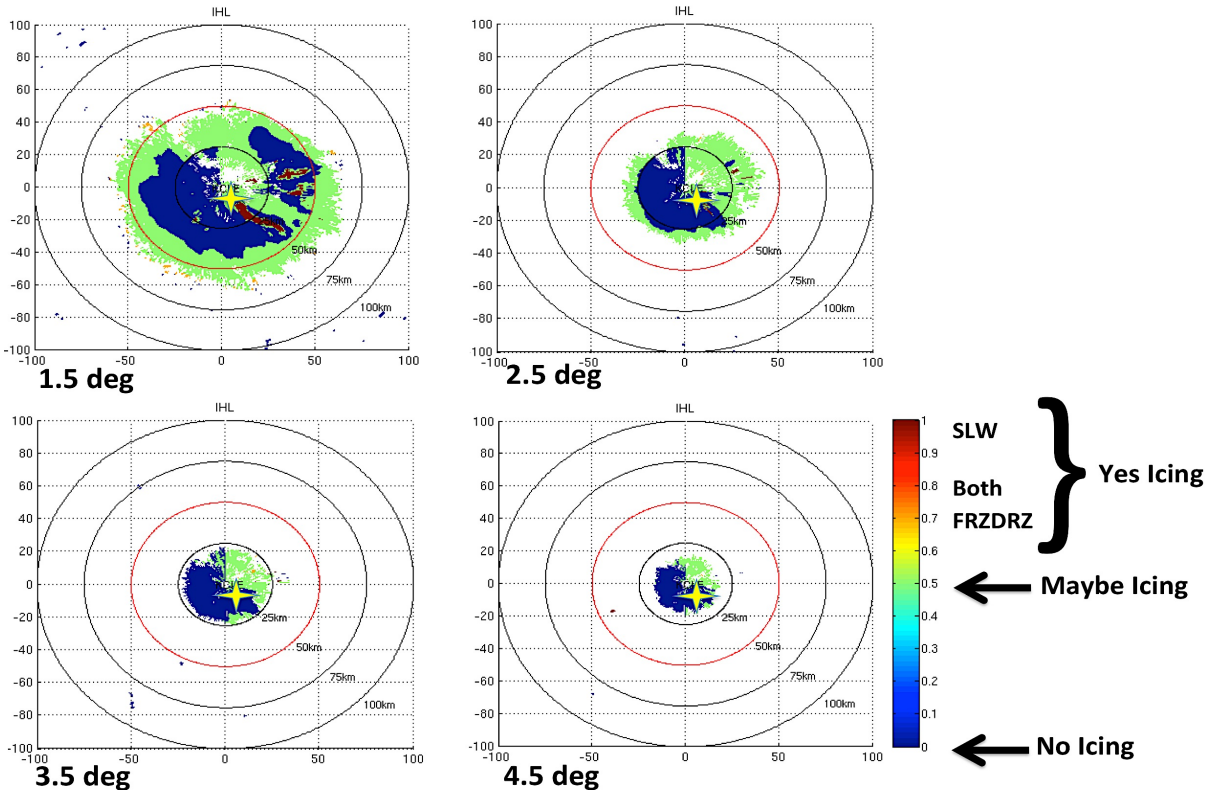

Figure 15. *KCLE IHLA output for elevations 1.5 to 4.5 degrees from 1728 UTC 12 February 2012. PIREP location is shown as a gold star.*

4.2 Overall Statistics

In this section, the overall statistics of the total study are described. For the KCLE IHLA radar volume analysis, the total results for both null and moderate or greater icing cases were recorded then averaged. These percentages will be shown in section 4.2.1. In addition, mean ILW comparisons to volumetric statistics are detailed in section 4.2.2.

4.2.1 Warning Volume Statistics

The total warning statistics methodology was described in section 3.2.3. For all the null and moderate or greater cases, a total mean percentage of radar volume of 'yes icing', 'SLW yes', 'FRZDRZ yes', 'maybe icing', and 'no icing' were recorded (Figure 16, top of next page). Figure 16 shows that for the 14 analyzed case dates with moderate or greater reported PIREP icing severities, 43.21 % of the operational radar volume was scored as 'yes icing', 8.56 % of the volume was scored as 'SLW yes', 34.65 % of the volume was scored as 'FRZDRZ yes', 43.65 % of the volume was scored 'maybe icing', and 13.14 % of the volume was scored 'no icing'. For the 17 analyzed case dates with null reported PIREP icing severities, 21.33 % of the operational radar volume was scored as 'yes icing', 12.51 % of the volume was scored 'SLW yes', 8.82 % of the volume was scored 'FRZDRZ yes', 43.53 % of the volume was scored 'maybe icing', and 35.14 % of the volume was scored 'no icing'. In the moderate or greater cases, the majority of the detected icing was from the FRZDRZ algorithm, but for the null icing cases, the majority of the detected icing pixels were from the SLW algorithm. An earlier study by Serke et al. (2012), showed the opposite result. This was a surprise to the authors, since the FRZDRZ algorithm is based upon just single polarized reflectivity, and SLW is based upon dual polarized moments of K_{DP} and Z_{DR}. The result indicates that there is a need for further analysis to possibly tune or separate the FRZDRZ and SLW algorithms and specifically analyze each case in real time over several radar volume scans. Overall, these statistics displayed that the IHLA was effective in detecting the known icing conditions using operational dual polarization NEXRAD data, and shows promise for the algorithm. In addition to analyzing each case from this study, further case analysis will be performed during the next winter season.

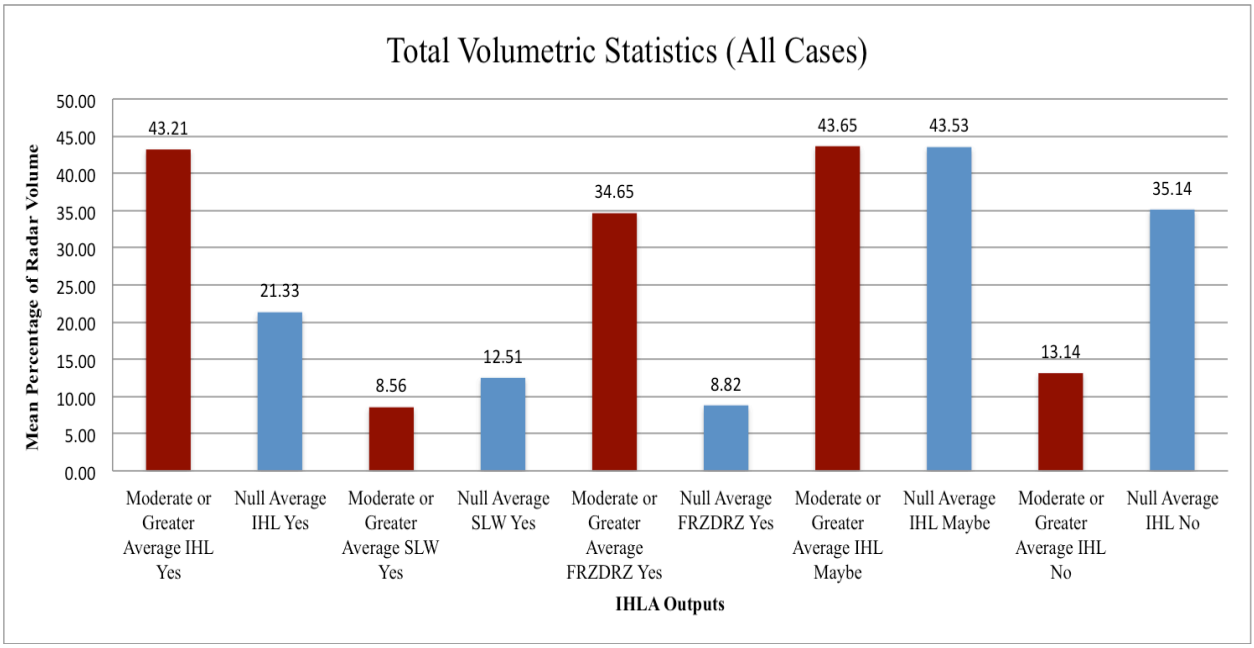

Figure 16. *Total warning volumetric statistics (all cases).*

4.2.2 Mean ILW Comparisons to Volumetric Statistics

The mean ILW comparison to volumetric statistics methodology was described in section 3.2.4. For all the null and moderate or greater cases, a scatterplot was made showing the mean radar volume percentages for IHLA 'yes icing' (section 3.2.3) versus 5-minute mean ILW values of NIRSS for each individual case (Figure 17, next page). The dots in the scatterplot represent the null PIREP cases and the stars represent the moderate or greater PIREP cases. The colors for each dot/star are separated into total pixels in the volume that had returned power above the signal-to-noise level. Red signifies the interval from 0 to 10,000 pixels, black signifies the interval from 10,000 to 25,000 pixels, pink signifies the interval from 25,000 to 50,000 pixels, blue signifies the interval from 50,000 to 100,000 pixels, and green signifies pixels greater than 100,000. A dashed line on Figure 17 represents a dividing line between where most of the moderate or greater icing cases and null icing cases lie. There were a few outliers for the moderate or greater cases, which lie below the dashed line. Figure 17 shows that for the 14 analyzed case dates with moderate or greater reported PIREP icing severities, the mean ILW value for all cases was 0.303 gm^{-3} and the mean radar volume percentage for IHLA 'yes icing' for all cases was 43.21 %. For the 17 analyzed case dates with null reported PIREP severities, the mean ILW value for the 17 cases was 0.089 gm^{-3} and the mean radar volume percentage for IHLA 'yes icing' for the 17 cases was 21.33 %.

Overall, these statistics displayed that the mean radar volume percentage for IHLA 'yes icing' for both null and moderate or greater icing cases matched reasonably with the mean 5-minute ILW values of NIRSS. The null cases were all below an ILW value of 0.200 gm^{-3}, which is the initial value for moderate icing severity for NIRSS. Eight of the fourteen (57 %) moderate or greater cases were above the threshold of moderate icing severity for NIRSS. The other 6 (43 %) were below the threshold, however, there were 4 out of those 6 that were near the 0.200 gm^{-3} ILW value. Both NIRSS and the IHLA did detect these cases reasonably well, but the scale of the SLW features aloft can quickly change over the vertically pointing system, thus causing the severity of NIRSS to not match certain cases.

5. CONCLUSION

In this work the authors showed that the idea of an in-flight icing hazard product utilizing dual polarized S-band research radar moment fields could be extended for use for the United States network of NEXRAD radars. The study looked at a series of icing and

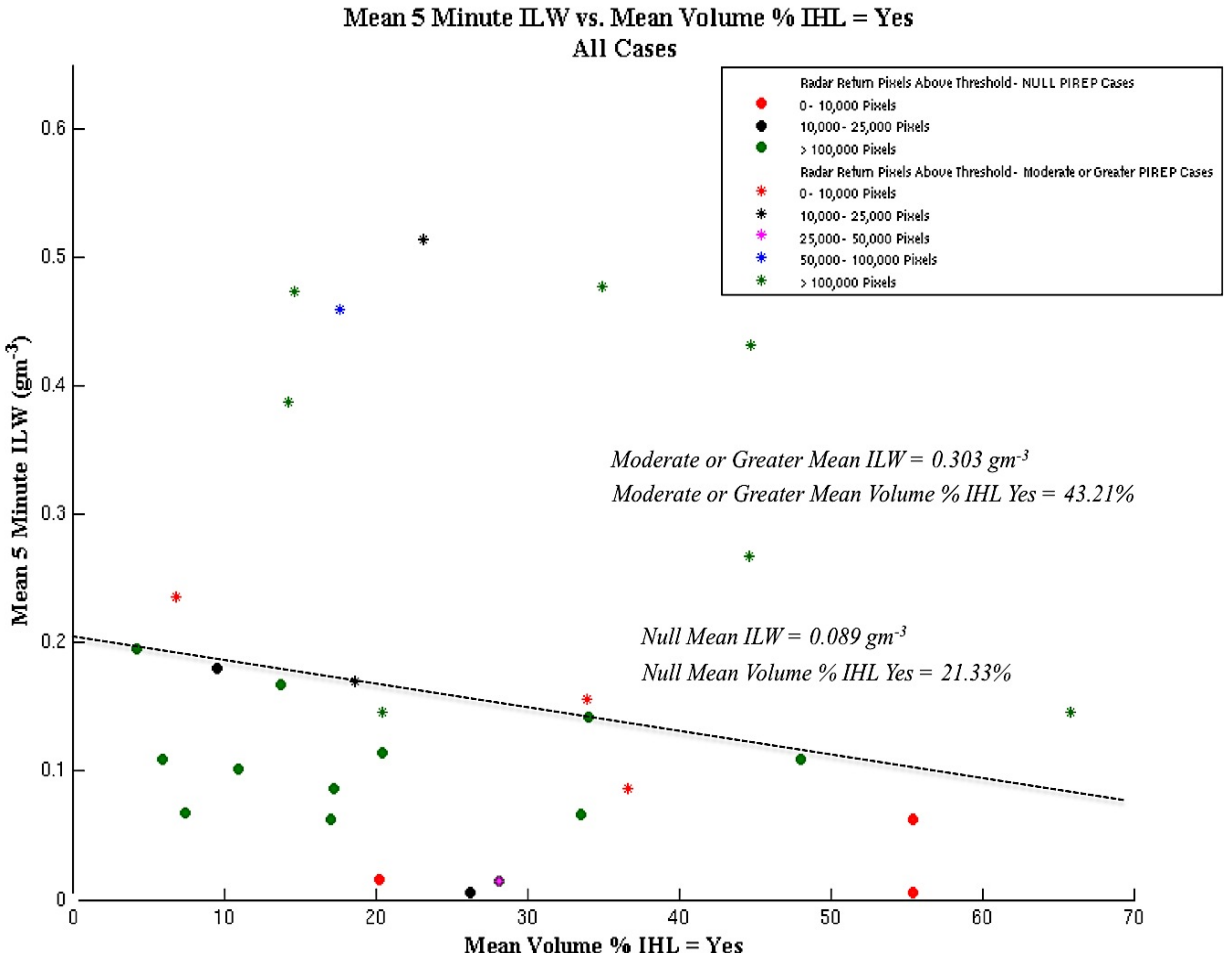

Figure 17*. Scatterplot of mean 5 Minute ILW vs. mean volume % IHLA = Yes (All cases).*

non-icing cases based upon PIREPs inside a 50 km radius of Cleveland, Ohio's dual-polarized radar (KCLE), from 27 January 2012 to 20 March 2012. Individual case studies of both a moderate and null PIREP were shown. For both the moderate and null icing case studies, the IHLA output near the location of the PIREP and mean warning volume percentages corresponded well with the known icing conditions. In addition, the SLW algorithm identified the in-flight icing condition for the moderate PIREP. Both cases, however, had a large percentage of 'icing maybe' which must be examined in a future analysis.

Next, overall warning volume statistics were calculated and shown. The statistics demonstrated that the IHLA was successful in detecting the known icing conditions and shows promise. A study by Serke et al. (2012) showed for a small number of case studies that the majority of detected icing for moderate or greater icing cases was from the SLW algorithm, while the majority of detected icing for the null icing cases was from the FRZDRZ algorithm. The findings in this particular study were contradictory, which indicates that there is a need for further analysis to possibly tune or separate the FRZDRZ and SLW algorithms, and specifically analyze each case in real time over several radar volume scans.

Lastly, mean ILW comparisons to volumetric statistics were made. Overall, these statistics displayed that the mean radar volume percentage for IHLA 'yes icing' for both null and moderate or greater icing cases matched reasonably with the mean 5-minute ILW values. There were however, outliers in the moderate or greater icing category, which could be due to the scale of SLW features aloft which could have changed rapidly over the vertically pointing NIRSS.

One major shortcoming of the IHLA technique is that S-band radars, even finely tuned research radars, are effectively precipitation radars and not cloud radars.

Cloud-sized drops, considered as those with diameters < 50 μm, are often not large enough to be detectable by these radars. Another noteworthy limitation to this polarized S-band method is related to biasing of the Z_{DR} field in the presence of canted particles. Z_{DR} cannot be calibrated by performing vertical scans with NEXRAD.

The best way to approach a volumetric warning system may be to extend the NIRSS icing products to cover the entire aircraft takeoff and landing space, which would ingest the operational S-band reflectivity. Both the IHLA and NIRSS have been proven to provide accurate detection of in-flight icing hazards for SLW. Combining the remotely sensed fields obtained from both products would be the most logical and economic approach to creating a volumetric icing hazard warning system. This research is a vital step towards demonstrating a feasible icing hazard algorithm.

6. ACKNOWLEDGEMENTS

This research is sponsored by the NASA Aviation Safety Program under the Atmospheric Environment Safety Technologies (AEST) project. The views expressed are those of the authors and do not necessarily represent the official policy or position of the NASA.

7. REFERENCES

Albo, D., S. Ellis, D. Serke, A. Weekley, D. Adriaansen, C. Johnston, M. Politovich, M. Dixon, and J. Hubbert, Icing Hazard Level: Final Report 2011-2012, *Report to MIT-LL and FAA*, 64 pp., 2012.

Brandes, E. and K. Ikeda, 2004: Freezing-Level Estimation with Polarimetric Radar. *J. Appl. Meteor.*, **43**, pp. 1541–1553.

Doviak, R. J., and D. S. Zrnić, 1993: *Doppler Radar and Weather Observations*. Academic Press. 562 pp.

Ellis, S. M., J. Vivekanandan, S. Goeke, E. A. Brandes, J. Stith, and R. J. Keeler, 2001: In-situ verification of remote aircraft icing detection using S-band polarization radar measurements. Preprints, *30th Int. Conf. On Radar Meteorology*, Munich, Germany, Amer. Meteor. Soc., 2B.6. Available online.

Elmore, K., 2009: Test and Evaluation of NSSL Hydrometeor Classification Algorithm in Winter Precipitation. *FAA Report*.

Glickman, T., Glossary of Meteorology. 2nd ed. Amer. Meteor. Soc., 855 pp., 2000.

Gourley, J. J., C. M. Calvert, 2003: Automated Detection of the Bright Band Using WSR-88D Data. *Wea. Forecasting*, **18**, 585–599.

Hubbert, J., S. Ellis, M. Dixon, and G. Meymaris, 2010: Modeling, error analysis and evaluation of dual-polarization variables obtained from simultaneous horizontal and vertical polarization transmit radar. Part I: Modeling and Antenna Errors. *J. Atmos. Ocean. Tech.*, **27**, pp. 1583-1598.

Hubbert, J., S. Ellis, M. Dixon, and G. Meymaris, 2010: Modeling, error analysis and evaluation of dual-polarization variables obtained from simultaneous horizontal and vertical polarization transmit radar. Part II: Experimental Data. *J. Atmos. Ocean. Tech.*, **27**, pp. 1599-1607.

Hydrometeorological Prediction Center. (2012). HPC's Surface Analysis Archive. Available from http://has.Ncdc.noaa.gov/pls/plhas/HAS.FileAppSelect?datasetName=6500

Ikeda, K., R. Rasmussen, E. Brandes, and F. McDonough, 2008: Freezing drizzle detection with WSR-88D radars. *J.Appl. Meteor. Climatol.*, **48**, pp. 41-60, 2008.

Johnston, C. J., D. J. Serke, D. R. Adriaansen, A. L. Reehorst, M. K. Politovich, C. A. Wolff, and F. McDonough 2011: Comparison of In-Situ, Model and Ground Based In-Flight Icing Severity. NASA/TM 2011-217141. NASA.

Jolliffe, I. and D. Stephenson, Forecast Verification: A Practitioner's Guide in Atmospheric Science. Wiley and Sons, Chichester, West Sussex, England. 240 pp., 2003.

National Climatic Data Center. (2012). Level II NEXRAD Data Online [Data File]. Available from http://has.ncdc.noaa.gov/pls/plhas/HAS.FileAppSelect?datasetName=6500

Park, H., A. Ryzhkov, D. Zrnić, and K. Kim, 2009: The Hydrometeor Classification Algorithm for the Polarimetric WRS-88: Description and Application to an MCS. *Wea. And Forecasting*, **24**, pp. 730-748.

Plummer, D. M., S. Göke, R. M. Rauber, and L. Di Girolamo, 2010: Discrimination of Mixed-versus Ice-Phase Clouds Using Dual-Polarization Radar with Application to Detection of Aircraft Icing Regions. *J. Appl. Meteor. Climatol.*, **49**, pp. 920–936.

Reehorst, A. L., D. J. Brinker, and T. P. Ratvasky, 2005: NASA Icing Remote Sensing System: comparisons from AIRS-II. NASA/TM-2005-213592. NASA.

Reehorst, A., M. Politovich, S. Zednik, G. Isaac, and S. Cober, 2006: Progress in the development of practical remote detection of icing conditions. NASA/TM-2006-214242, NASA.

Rinehart, R.E., 2010: *Radar for Meteorologists*. Rinehart Publishing, Nevada, Missouri, USA.

Rogers, R. R., and M. K. Floyd: A Short Course in Cloud Physics. Pergamon Press, Oxford, England.

Serke, D. J., S. M. Ellis, A. Reehorst., J. Hubbert, D. Albo, A. Weekley, D. Adriaansen, C. Johnston, and M. Politovich, 2012: Progress toward a volumetric in-flight icing hazard system for airports which incorporates operational dual-polarization S-band radars. The Seventh European Conference on Radar Conference on Radar in Meteorology and Hydrology, Toulouse, France, June 24-29. Available online.

Solheim, F., J. Godwin, E. Westwater, Y. Han, S. Keihm, K. Marsh, and R. Ware, 1998: Radiometric profiling of temperature, water vapor and cloud liquid water using various inversion methods. *Radio Sci.*, **33**, pp. 393-404, 1998.

Vivekanandan, J., S.M. Ellis, R. Oye, D. S. Zrnić, A. V. Ryzhkov, and J. Straka, 1999: Cloud Microphysics Retrieval Using S-band Dual-Polarization Radar Measurements. *Bull. Amer. Meteor. Soc.*, **80**, pp. 381-388.

Wheeler, M., Report on the Radar/PIREP Cloud Top Discrepancy Study, NASA Contractor Report CR-204381, Applied Meteorology Unit, ENSCO, Inc., 1980 N. Atlantic Ave, Cocoa Beach, FL 32931, 18 pp., 2007.

Wilks, D., Statisitcal Methods in the Atmospheric Sciences. Academic Press, New York, NY. 627 pp., 2006.

Williams, E. R., D. J. Smalley, M. F. Donovan, R. G. Hallowell, K. T. Hood, B. J. Bennett, R. Evaristo, A. Stepanek, T. Bals-Elsholz, J. Cobb, and J. M. Ritzman, 2011: Dual polarization radar winter storm studies supporting development of NEXRAD-based aviation hazard products. AMS 35th Conf. on Radar Meteorology, Pittsburgh, PA, 26-30 September.

8. APPENDIX

8.1 Acronyms

8.1.1 Radar Moment Fields

K_{DP} - 'Specific Differential Phase' – range derivative of differential phase (see ϕ_{DP})

ϕ_{DP} - 'Differential Phase' – measured difference in horiz. and vert. pulse phase shift

LDR - 'Linear Depolarization Ratio'

dBZ - 'Reflectivity', single-polarimetric

ρ_{HV} - 'Correlation coefficient'

Z_{DR} - 'Differential Reflectivity' – ratio of returned horizontal and vertical power

8.1.2 Algorithms

FRZLA - 'Freezing Level Algorithm', (see Albo et al., 2012)

FRZDRZ - 'Freezing Drizzle Algorithm', (see Ikeda et al., 2009)

HCA - 'Hydrometeor Classification Algorithm'

IHLA - 'Icing Hazard Level Algorithm', (see Albo et al., 2012)

PID - legacy 'Particle Identification' algorithm (see Vivekanandan et al., 1999)

SLW - 'Supercooled Liquid Water Algorithm', (see Plummer et al., 2010)

8.1.3 Miscellaneous

CSU-CHILL - 'Colorado State University/ University of CHicago, ILLinois' scanning 10-cm wavelength S-band polarized radar located in Greeley, CO

ILW- 'integrated liquid water'

KCLE - call letters for Cleveland's Hopkins International Airport operational radar and ASOS

KDEN - call letters for Denver's International Airport

KOUN - call letters for Oklahoma University's polarized S-band research radar

MSL - 'mean sea level'

NCAR - 'National Center for Atmospheric Research'

NEXRAD - 'NEXt generation RADar', or S-band WSR-88D radar

NIRSS - 'NASA Icing Remote Sensing System'

NOAA - 'National Oceanic and Atmospheric Administration'

NSSL - 'National Severe Storms Laboratory'

NWP - 'Numerical Weather Prediction'

PIREP(s) - 'PIlot REPort'

PSS - 'Peirce Skill Score'

RCS - 'Radar Cross-section'

SLW - 'Supercooled Liquid Water'

WRF-RR - 'Weather Research and Forecast Rapid Refresh' numerical weather prediction model

8.2 Pilot Reports

8.2.1 Null Pilot Report

2/12/12
1721 1329067260 41.36 -81.77 40 38 8 55 55 0 600 -9 -9 -14 -99 -99 40 40 -1 -9 55 600 -1 -9 40 40 -9 –9 -9 40 40 -9 -9 -9 E145 CLE UA/OV CLE135005 /TM 1721 /FL040 /TP E145 /SK OVC038-TOP055/ SKC /TA M14 /IC NEG

8.2.2 Moderate Pilot Report

02/02/12
1408 1328191680 41.65 -81.54 60 -9-9 -9 -9-9 -9-9-9 -9-99-99 60 60 4-9 60 60 5-9 60 60-9-9-9 60 60-9-9-9F900CGFUA /OV CLE045020 /TM 1408 /FL060 /TP F900 /TA M09 /IC LGT-MOD 070-060 MOD 040-030 LGT 020-BLO /RM DURD

8.3 Tables

Category	Name	Description	Value	Icing
1	High SLW	SLWA output >0.55	1.0	Yes
2	High FZDZ	MNDDA output >0.70	0.7	Yes
3	Both high	Category 1 and 2 apply	0.8	Yes
4	Both low	SLWA and MNDDA output both <0.45	0.0	No
5	Below SNR	When mean dBZ < -31 dBZ	-0.1	Unknown
6	Both medium	Not categories 1 through 5	0.5	Maybe

Table 1. Icing hazard values sorted into various output categories (Albo et al., 2012).

Null PIREPs						
Date	Time	Average 5 Minute ILW (gm^{-3})	NIRSS Severity	Radar Return Pixels Above Threshold	Pixels Where IHL = Yes	Mean Volume % IHL Yes
20120204	20:57 UTC	0.006	No Icing	19111	5007	26.20%
20120208	11:10 UTC	0.066	Trace	873250	293174	33.57%
20120208	13:14 UTC	0.110	Light	1178717	565810	48.00%
20120208	15:51 UTC	0.142	Light	1085658	369675	34.05%
20120208	21:27 UTC	0.014	No Icing	178919	50428	28.18%
20120211	15:18 UTC	0.102	Light	2011470	220314	10.95%
20120211	16:13 UTC	0.062	Trace	2066357	352179	17.04%
20120211	19:36 UTC	0.114	Light	1642055	335153	20.41%
20120212	02:18 UTC	0.168	Light	196312	27029	13.77%
20120212	16:24 UTC	0.068	Trace	470323	34960	7.43%
20120212	17:24 UTC	0.196	Light	522050	21956	4.21%
20120212	20:25 UTC	0.016	No Icing	2706	548	20.25%
20120215	17:56 UTC	0.006	No Icing	3580	1984	55.42%
20120219	15:21 UTC	0.062	Trace	9012	4996	55.44%
20120221	19:08 UTC	0.180	Light	20606	1969	9.56%
20120222	15:12 UTC	0.086	Trace	143630	24805	17.27%
20120223	22:57 UTC	0.110	Light	563657	33614	5.96%

Table 2. Null icing cases – mean ILW comparisons to volumetric statistics.

Moderate or Greater PIREPs						
Date	Time	Average 5 Minute ILW (gm^{-3})	NIRSS Severity	Radar Return Pixels Above Threshold	Pixels Where IHL = Yes	Mean Volume % IHL = Yes
20120127	12:12 UTC	0.388	Heavy	492632	70181	14.25%
20120202	14:11 UTC	0.432	Heavy	276372	123593	44.72%
20120202	21:35 UTC	0.170	Light	10111	1885	18.64%
20120207	15:15 UTC	0.236	Moderate	5812	396	6.81%
20120207	22:04 UTC	0.478	Heavy	269841	94412	34.99%
20120208	03:10 UTC	0.268	Moderate	249665	111387	44.61%
20120210	17:11 UTC	0.146	Light	1249844	823319	65.87%
20120214	19:37 UTC	0.460	Heavy	68153	12012	17.63%
20120222	02:06 UTC	0.474	Heavy	120870	17693	14.64%
20120222	22:34 UTC	0.146	Light	235402	48108	20.44%
20120224	16:45 UTC	0.282	Moderate	35946	5098	14.18%
20120224	22:30 UTC	0.514	Heavy	24506	5684	23.19%
20120225	22:41 UTC	0.086	Trace	3489	1278	36.63%
20120226	00:06 UTC	0.156	Light	3828	1299	33.93%

Table 3. Moderate or greater icing cases – mean ILW comparisons to volumetric statistics.